

SURGE: Continuous Detection of Bursty Regions Over a Stream of Spatial Objects

Kaiyu Feng, Tao Guo, Gao Cong^{ID}, Sourav S. Bhowmick^{ID}, and Shuai Ma^{ID}

Abstract—With the proliferation of mobile devices and location-based services, continuous generation of massive volume of streaming spatial objects (i.e., geo-tagged data) opens up new opportunities to address real-world problems by analyzing them. In this paper, we present a novel *continuous bursty region detection* (SURGE) problem that aims to continuously detect a *bursty region* of a given size in a specified geographical area from a stream of spatial objects. Specifically, a bursty region shows maximum spike in the number of spatial objects in a given time window. The SURGE problem is useful in addressing several real-world challenges such as surge pricing problem in online transportation and disease outbreak detection. To solve the problem, we propose an exact solution and two approximate solutions, and the approximation ratio is $\frac{1-\alpha}{4}$ in terms of the burst score, where α is a parameter to control the burst score. We further extend these solutions to support detection of *top-k bursty regions*. Extensive experiments with real-world data are conducted to demonstrate the efficiency and effectiveness of our solutions.

Index Terms—Spatial data, data stream, burst detection, region detection

1 INTRODUCTION

PEOPLE often share geo-tagged messages through many social services like *Twitter* and *Facebook*. Each geo-tagged data is associated with a timestamp, a geo-location, and a set of attributes (e.g., tweet content). In this paper, we refer to them as *spatial objects*. With the proliferation of GPS-enabled mobile devices and location-based services, the amount of such spatial objects (e.g., geo-tagged tweets and trip requests from *Uber*) is growing at an explosive rate. Their real-time nature coupled with multi-faceted information and rapid arrival rate in a streaming manner open up new opportunities to address real-world problems. For example, consider the following problems.

Example 1. The world regularly faces the challenge of tackling a variety of virus epidemics such as SARS, MERS, Dengue, and Ebola. For example, the outbreak of mosquito-borne Zika virus started in Brazil in 2015. It is of interest to continuously monitor different areas for possible Zika outbreak and issue alerts to people who are traveling to or living in regions affected by Zika. Since early detection of such outbreak is paramount, how can we identify potential Zika-affected region(s) in real time?

One strategy to address this issue is to continuously monitor geo-tagged tweets (i.e., spatial objects) coming out of a specific area (e.g., Florida) and detect regions where there are sudden bursts in tweets related to Zika (e.g., containing Zika-related keywords) in real time. Observe that these “bursty regions” are dynamic in nature. However, it is computationally challenging to continuously monitor massive streams of spatial objects and detect bursty regions in real time.

Example 2. Online transportation network companies such as *Uber*, *Lyft*, and *Didi Dache* have disrupted the traditional transportation model and have gained tremendous popularity among customers.¹ Customer can submit a trip request through their mobile apps. If a nearby driver accepts the request, he will pickup the customer.

Although this disruptive model has benefited many drivers and customers, the latter may have to wait for a long time for a car when the number of car requests significantly surpasses the supply of nearby drivers. Clearly, it is beneficial to both passengers and drivers if we can notify idle drivers in real time whenever there is a sudden burst of consumer demand in areas of interest to them. An additional benefit to the drivers is that the trip fare may be increased due to the “surge pricing” policy² where the companies may increase a trip price significantly when demand is high. For instance, consider Fig. 1, which shows the trip requests in two time windows $[t_1, t_2]$ and $[t_2, t_3]$. Suppose a driver is only interested in the area shown by dashed rectangle to pick up passengers. Observe that there

• K. Feng, T. Guo, G. Cong, and S.S. Bhowmick are with the School of Computer Science and Engineering, Nanyang Technological University, 639798 Singapore.

E-mail: {kfeng002, tguo001}@e.ntu.edu.sg, {gaocong, assourav}@ntu.edu.sg.

• S. Ma is with the SKLSDELab, School of Computer Science and Engineering, Beihang University, Beijing 100091, China, and Beijing Advanced Innovation Center for Big Data and Brain Computing, Beijing, China.

E-mail: mashuai@buaa.edu.cn.

Manuscript received 11 Mar. 2018; revised 18 Sept. 2018; accepted 22 Apr. 2019. Date of publication 8 May 2019; date of current version 6 Oct. 2020.

(Corresponding authors: Gao Cong and Shuai Ma.)

Recommended for acceptance by W. Wang.

Digital Object Identifier no. 10.1109/TKDE.2019.2915654

1. In 2017, Uber is available in over 81 countries and 570 cities worldwide.

2. For example, the price increased 10X on new year’s eve in 2016 in the United States (www.geekwire.com/2016/customers-complain-uber-prices-surge-near-10x-new-years-eve/)

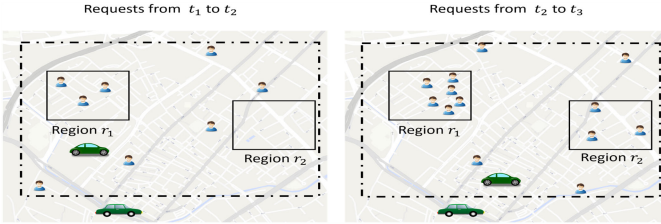


Fig. 1. Motivating example.

is a burst of trip requests in regions r_1 and r_2 (both increased by 3). If the app can notify the driver in real time about these two regions, then he can move in there to pickup potential passengers. Note that such soaring demand is not always predictable as it may not only occur during holidays or periodic events (e.g., new year's eve) but also due to unpredictable events such as subway disruption, concerts, road accident, inclement weather, and terrorist attack.

There are two common themes in the two examples. First, we need to continuously monitor a large volume of spatial objects (e.g., trip requests and geo-tagged tweets) to detect in real time one or more regions that show relatively large spike in the number of spatial objects (i.e., bursty region) in a given time window. Second, a user needs to specify as input the size $a \times b$ of rectangular-shaped bursty region that one wishes to detect. For instance, in Example 2 different drivers may prefer bursty regions of different sizes according to their convenience.

In this paper, we refer to the problem embodied in the aforementioned motivating examples as *continuous bursty region detection* (SURGE) problem. Specifically, given a region size $a \times b$ and an area A , the aim of the SURGE problem is to continuously detect a region of the specified size in A that demonstrates the *maximum burstiness* from a stream of spatial objects. To model the burstiness of a region, we propose a general function based on the sliding window model. We also extend our SURGE problem to detect *top-k* bursty regions as in certain applications one may be interested in a list of such regions.

The SURGE problem and its *top-k* variant are challenging as we need to handle rapidly arriving spatial objects in high volume to efficiently detect and maintain bursty regions. For example, 10 million geo-tagged tweets are generated each day in *Twitter*.³ As we shall see later, it is prohibitively expensive to recompute bursty regions frequently.

In this paper, we first propose an exact solution called *cell-cSPOT* to keep track of the bursty region over sliding windows. Specifically, we first reduce the SURGE problem to *continuous bursty point detection* (cSPOT) problem. Then we propose a cell-based algorithm to continuously detect the bursty point. It takes $O(|c_{max}|^2 + \log n)$ time to process a new arriving spatial object on average, where $|c_{max}|$ is the maximum number of objects that we search inside a cell, and n is the number of indexed rectangle objects.

Although *cell-cSPOT* can address the SURGE problem efficiently in several scenarios, it becomes inefficient as $|c_{max}|$ increases (e.g., the sliding windows get larger, the region

size gets larger, or the arrival rate of the spatial objects increases). To address this we further propose two approximate solutions, namely GAP-SURGE and MGAP-SURGE, with a complexity of $O(\log n)$ to process a spatial object. The approximation ratio is bounded by $\frac{1-\alpha}{4}$, where $\alpha \in [0, 1]$ is a parameter used in the *burst score function*. Last, we show that our proposed solutions can be elegantly extended to continuously detect top- k bursty regions. Our experiments reveal that our proposed solutions can handle streams with up to 10 millions spatial objects arrived per day.

In summary, this paper makes the following contributions:

- 1) We propose a novel *continuous bursty region detection* problem for continuously detecting bursty regions in a specified area from a stream of spatial objects. (Section 3)
- 2) We present an exact solution (*cell-cSPOT*) and two approximate solutions (GAP-SURGE and MGAP-SURGE) to address the SURGE problem (Sections 4 and 5). We further extend these solutions to keep track of top- k bursty regions efficiently (Section 6).
- 3) We conduct experiments with real-world datasets to show the efficiency of our proposed solutions. All solutions are efficient in real time. Moreover, GAP-SURGE and MGAP-SURGE scale well w.r.t. high arrival rate while the returned regions have competitive burst scores. The extended versions can also detect top- k bursty regions efficiently in real time. (Section 7).

The proofs of lemmas and theorems are given in Appendix.

2 RELATED WORK

Burst Detection. Our SURGE problem is related to the problem of detecting bursty patterns and topics. A host of work has been done to detect temporal bursts [2], [9], [13], [21], [26]. A collection of proposals focus on detecting bursty features (represented by probability distribution of words) [9], [13], [21]. The other work focuses on detecting a timespan over the stream such that its aggregate is larger than a threshold [2], [26]. All these burst detection problems are different from our SURGE problem as they disregard the spatial information when detecting the temporal bursts.

Most germane to our work are efforts on exploring spatial-temporal bursts [14], [17], [25] albeit from different aspects. Mathioudakis et al. [17] study the problem of identifying notable spatial burst out of a collection of user generated information. They divide the space into cells, and recognize two states for each cell, namely “bursty” and “non-bursty”. Our SURGE problem differs from it in two key aspects. First, the spatial burst is identified as a cell in the grid whereas the bursty region in SURGE can be located at any position. Second, the solution developed in [17] is designed for data stored in a data warehouse, and it cannot be deployed or adapted to solve the SURGE problem. Given a set of geo-tagged text streams, Lappas et al. [14] study the problem of identifying a combination of a temporal interval and a geographical region with unusual high frequency for a term. Though it adopts a similar score function to model the burstiness, it is a different problem from SURGE: They aim to detect regions that maximize the burstiness without any size constraint. They would expand the bursty region to include a geo-tagged text stream

3. <https://www.mapbox.com/blog/twitter-map-every-tweet/>

as long as it is bursty, i.e., the term in this stream in a recent time period is more frequent than expected. Therefore, users cannot specify the size of the detected bursty region a priori. In contrast, SURGE allows users to specify the size of the bursty region that they want to detect for applications like Example 2. Hence, we cannot adopt the proposed technique [14] to solve the SURGE problem. Given a geo-tagged tweet stream, Zhang et al. [25] aim to continuously detect real-time local event. Specifically, a local event is defined as a cluster of tweets that are semantically coherent and geographically close. Our problem differs from it in the following aspects. First, the bursty event is identified as a cluster of geo-tagged tweets, while our SURGE problem aims to detect a spatial region. Second, the proposed framework is built over geo-textual stream. The textual content serves as an important feature in their system. Our SURGE is applicable to any kind of spatial stream.

Dense Region Search. Our problem is also related to dense region search over moving objects [12], [19]. Given a set of moving objects, whose positions are modeled as linear functions in Euclidean space, the dense region search problem aims to find all dense regions at query time t . Jensen et al. [12] constraint dense regions to be non-overlapping square-shaped regions of given size, whose density is larger than a user-specified threshold. Ni et al. [19] propose a new definition of dense regions, which may have arbitrary shape and size. In the dense region search problem, the positions of the moving objects are modeled as linear functions. Thus the position of each moving object can be computed at any time. In contrast, in the SURGE problem, the number of the newly-arriving spatial objects and their positions are unknown a priori. Moreover, the density function is different from our burst score function, requiring different techniques to compute the burst score of a given region.

Region Search. Our problem is also related to the region search problem. A class of studies aims to find a region of a given size such that the *aggregation score* of the region is maximized [6], [7], [18], [20]. Given a set of spatial objects, the *max-enclosing rectangle* (MER) problem [18] aims to find the position of a rectangle of a given size $a \times b$ such that the rectangle encloses the maximum number of spatial objects. This problem is systematically investigated as the *maximizing range sum* (*MaxRS*) problem [6], [20]. Feng et al. [7] further study a generalized problem of the *MaxRS* problem, in which the aggregate score function is defined by submodular monotone functions, which include sum. Liu et al. [16] study the problem of finding subject oriented top- k hot regions, which can be considered as a top- k version of the *MaxRS* problem. Cao et al. [3] study the problem of finding a subgraph of a given size with the maximum aggregation score from a road network. All these aforementioned region search problems focus on static data. Moreover, the idea of invoking the approach designed for the region search problem whenever a object enters or leaves the sliding windows is prohibitively expensive (We will elaborate on this in Section 4.3).

Our work is closely related to the recent efforts on continuous *MaxRS* problem [1], [11]. Amagata et al. [1] propose the problem of monitoring the *MaxRS* region over spatial data streams. Specifically, given a stream of weighted spatial objects, the continuous *MaxRS* problem aims to monitor the location of a rectangle of a size $a \times b$ such that the sum of the

weights of the objects covered by the rectangle is maximized. In the proposed algorithm, a grid is imposed over the space, whose granularity is independent from the size of the query rectangle. For each spatial object in the stream, they generate a rectangle of a size $a \times b$ whose center is located at the spatial object. The generated rectangle is mapped to the cells with which it overlaps. For each cell, they maintain a graph where each node in the graph is a rectangle mapped to this cell, and two nodes are connected by a directed edge if they overlap with each other. The graph is used to handle the updates of the stream. For each rectangle in the cell, they maintain an upper bound to determine when to invoke the sweep-line algorithm [18] to find the most overlapped region inside the rectangle. With the maintained upper bounds, they use a branch-and-bound algorithm to reduce the search space. The difference of the SURGE problem from the continuous *MaxRS* problem is that the burst score of the SURGE problem is defined over two consecutive sliding windows, and spatial objects in different windows contribute differently to the burst score. Though their solution cannot be directly applied to solve the SURGE problem, we can adapt their solution with some modifications for the SURGE problem. One issue of this solution is that they need to maintain a graph for each cell with a space cost of $O(n^2)$, where n is the number of rectangle objects that are mapped to the cell. When the number of objects mapped to a cell is large, the space cost could be extremely high. We will show in Section 7.2 that our proposed solutions outperform the *aG2* algorithm for the SURGE problem. Hussain et al. [11] investigates the *MaxRS* problem on the trajectories of moving objects. Given the trajectories of a set of moving points, they aim to maintain the result of the *MaxRS* problem at any time instant. Its problem setting is different from ours: it takes as input the trajectories of a set of fixed number moving objects, while in SURGE, the number of spatial objects in the sliding windows may vary with time and the positions of the newly arrived objects are unknown a priori.

This work is an extension of our previous work [8], where we introduce the SURGE problem and present an exact solution. In this paper, we propose two approximation algorithms to address the SURGE problem with an approximation ratio of $\frac{1-\alpha}{4}$, where $\alpha \in [0, 1]$ is a parameter used in the *burst score function*. Second, as in certain applications users may be interested in a list of bursty regions, we propose a top- k variant of the SURGE problem, and extend all the three algorithms to keep track of top- k bursty regions efficiently. Finally, we conduct extensive experiments to evaluate the three algorithms and include a case study to evaluate the quality of the exact solution.

Data Stream Management. Our work is also related to data stream management. There has been a long stream of work on various aspects of data streams since the last decade and we only review the work that involves spatial information. Given a stream of spatial-textual objects, [23] aims to estimate the cardinality of a spatial keyword query on objects seen so far. A host of work has also been done to study content-based publish/subscribe systems [4], [5], [10], [15], [22], [24] over spatial object streams. In these systems, streaming published items are delivered to the users with matching interests. However, none of these studies consider the problem of detecting bursty regions.

3 PROBLEM STATEMENT

3.1 Terminology

A *spatial object* is represented with a triple $o = \langle w, \rho, t_c \rangle$, where w is the weight of o , ρ is a location point with latitude and longitude, and t_c is the creation time of object o . In this paper, we consider a stream of spatial objects. For example, geo-tagged tweets in *Twitter* can be viewed as a stream of spatial objects arriving in the order of creation time. The *weight* of a tweet could be the relevance of its textual content to a set of query keywords. The car requests in *Uber* can also be viewed as a stream of spatial objects arriving in the order of calling time. In this case, the weight could be the passenger number or travel fare.

We next introduce two consecutive time-based sliding windows, namely *current* and *past windows*. Given a window size $|W|$, the *current window*, denoted by W_c is a time period of length $|W|$ that stretches back to a time $t - |W|$ from present time t . The *past window*, denoted by W_p is a time period of length $|W|$ that stretches back to a time $t - 2|W|$ from the $t - |W|$.

Given a region r and a sliding window W , let $O(r, W)$ be the set of spatial objects which are created in W and located in region r , i.e., $O(r, W) = \{o | o.\rho \in r \wedge o.t_c \in W\}$. Let $f(r, W)$ be the total weights of objects in $O(r, W)$ normalized by W 's length, i.e., $f(r, W) = \frac{\sum_{o \in O(r, W)} o.w}{|W|}$, which is the score of a region r w.r.t. the sliding window W .

Note that in this paper, for the sake of simplicity, we assume the current and the past windows have the same length $|W|$. However, our proposed solution is equally applicable when the two sliding windows have different lengths.

3.2 Burst Score

Intuitively, the *burst score* of a region r reflects the variation of the spatial objects in r in a recent period. This motivates us to design the burst score based on the current and past windows.

We first discuss the intuition in designing the *burst score* using Example 2. In this scenario, *Uber* drivers are interested in regions in which they have a higher chance to pick up a passenger. Obviously, a driver is more likely to find a passenger in a region that contains a large number of requests in the current window, which represents the *significance* of the region. On the other hand, if a region suddenly experiences a surge of requests, which represents the *burstiness* of the region, then it is highly likely that existing drivers in that region may not be able to fulfill this sudden increase in demand. Consequently, a driver will have a higher chance to find a passenger there.

Thus, we consider the following two factors in our burst score: (a) The score of the region w.r.t. the current window, i.e., $f(r, W_c)$, which measures the *significance*, and (b) the increase in the score of the region between the current window and the past window, i.e., $\max(f(r, W_c) - f(r, W_p), 0)$, which measures the *burstiness*. Note that we use the *max* function to guarantee that the increase in the score between the current and past windows is always non-negative since we are only interested in increase in the score.

We now formally define the burst score as follows.

Definition 1 (Burst Score). Given a region r , we define its burst score $S(r)$ as

$$S(r) = \alpha \max(f(r, W_c) - f(r, W_p), 0) + (1 - \alpha)f(r, W_c), \quad (1)$$

where $\alpha \in [0, 1]$ is a parameter that balances the significance and the burstiness.

3.3 Continuous Bursty Region Detection (SURGE) Problem

We are now ready to formally define the SURGE problem.

Definition 2 (Continuous Bursty Region Detection (SURGE) Problem). Consider a stream of spatial objects \mathcal{O} . Let $q = \langle A, a \times b, |W| \rangle$ be a SURGE query where A is a preferred area, $a \times b$ is the size of the query rectangle, and $|W|$ is the length of the current and past windows. Given such a query q , the aim of the SURGE problem is to continuously detect the position of the region r of size $a \times b$ in A with the maximum burst score. The region r is referred to as the *bursty region*.

4 AN EXACT SOLUTION

The SURGE problem is challenging to address due to the following reasons. First, given a snapshot of the stream, we are required to locate the bursty region in the preferred area A . Intuitively, this bursty region can be located at any point and it is prohibitively expensive to check the region located at every point, which is infinite. Second, whenever a spatial object enters or leaves the sliding windows, the burst score of any region which encloses this object may change. This implies that the location of the bursty region may change as well and we need to recompute the new bursty region. With the high arrival rate of the stream, it demands an efficient strategy to update the bursty region.

In this section, we present a solution to address the SURGE problem. We first introduce the *continuous bursty point detection* problem in Section 4.1. We show that by reducing the SURGE problem to the cSPOT problem, for any snapshot of the stream, we convert the challenge of selecting a point from infinite points in the preferred area A to selecting a *bursty point* from $O(n^2)$ disjoint regions. To address the second challenge, we present a cell-based algorithm to continuously update the *bursty point* in Section 4.3.

4.1 The cSPOT Problem

We next define the cSPOT problem and present how to reduce the SURGE problem to the cSPOT problem. First, we introduce some terminologies that will be used to define the cSPOT problem.

Definition 3 (Rectangle Object). A rectangle object, denoted with a triple $g = \langle w, \rho, t_c \rangle$, is a rectangle of size $a \times b$, where $g.w$ is its weight, $g.\rho$ is the location of its left-bottom corner, and $g.t_c$ is the creation time of g .

Given the stream of spatial objects \mathcal{O} , each spatial object o in \mathcal{O} can be mapped to a rectangle object g by using o as the left-bottom corner, i.e., $g.w = o.w$, $g.\rho = o.\rho$, and $g.t_c = o.t_c$. Let \mathcal{G} denote the stream of rectangle objects that are mapped from \mathcal{O} . Let $G(p, W)$ be the set of rectangle objects which covers point p and is created in window W , i.e., $G(p, W) = \{g | g.t_c \in W \wedge p \in g \wedge g \in \mathcal{G}\}$.

Next, we define the burst score of a point by following the definition of burst score of a region in Section 3 . With a

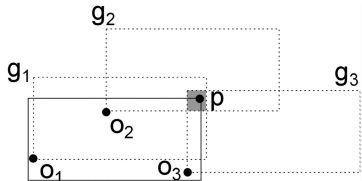


Fig. 2. Reduce to cSPOT problem.

slight abuse of notation, we continue to use $f(p, W)$ and $S(p)$ to denote the score of a point p w.r.t. the window W , and the burst score of p , respectively.

Definition 4 (Burst Score of a Points). Consider a stream of rectangle objects \mathcal{G} . The burst score $S(p)$ of point p is

$$S(p) = \alpha \max(f(p, W_c) - f(p, W_p), 0) + (1 - \alpha)f(r, W_c),$$

where $f(p, W)$, the score of a point p w.r.t. W , is the total weights of rectangle objects in $G(p, W)$ normalized by $|W|$, i.e., $f(p, W) = \frac{\sum_{g \in G(p, W)} g.w}{|W|}$.

We are now ready to formally define the cSPOT problem.

Definition 5 (cSPOT Problem). Consider a stream of rectangle objects \mathcal{G} , a parameter α , as well as the current window W_c and past window W_p . The Continuous Bursty Point Detection problem aims to keep track of a point p in the space, such that its burst score $S(p)$ is maximized. A point p with the maximum score is referred to as bursty point.

In order to reduce the SURGE problem to the cSPOT problem, for each spatial object o in the SURGE problem, if o is in the preferred area A , i.e., $o.\rho \in A$, we generate a rectangle object g of size $a \times b$ with o as the left-bottom corner such that $o.t_c = g.t_c$ and $g.\rho = o.\rho$. We illustrate this reduction with the example in Fig. 2. Assume that o_1, \dots, o_3 are all in A . For each spatial object $o_i, i \in [1, 3]$, a corresponding rectangle object g_i is generated. We next show the relationship between the bursty region and the bursty point of the corresponding SURGE and cSPOT problem.

Theorem 1. Let p_m be a bursty point for the reduced cSPOT problem given a snapshot. The rectangular region r_m of size $a \times b$ whose top-right corner is located at p_m is a bursty region for the original SURGE problem for the snapshot.

Note that the reduction is inspired by the idea of transforming the max-enclosing rectangle problem to the rectangle intersection problem [18]. The rectangle intersection problem aims to find the most overlapped area given a set of rectangles. Since our problem has a different burst score function, the techniques designed for the rectangle intersection problem cannot be utilized to search for the bursty point at a snapshot.

We address the SURGE problem by solving the corresponding cSPOT problem. Observe that in the cSPOT problem, the edges of the rectangle objects divide the space into many disjoint regions. Consider the example in Fig. 2. The shaded area is one of the disjoint region which is the overlap of g_1, g_2 , and g_3 . All points in a disjoint region are covered by the same set of rectangles. Thus they have the same burst score. Next we present a theorem which justifies the reason behind the reduction.

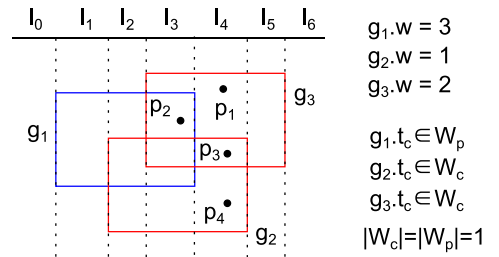


Fig. 3. Illustration of bursty point detection.

Theorem 2. Given a snapshot of the stream of rectangle objects in the cSPOT problem, there are at most $O(n^2)$ disjoint regions, where n is the number of rectangle objects in windows W_c and W_p [18].

Since all points in a disjoint region have the same burst score, Theorem 2 tells us that we only need to consider $O(n^2)$ disjoint regions, which addresses the first challenge of the SURGE problem, i.e., locating the bursty region from infinite possible locations.

Example 3. Consider a snapshot of the stream shown in Fig. 2. Assume that o_1, o_2 and o_3 are three spatial objects in the current window W_c in the SURGE problem, and $o_i.w = 1$ for $i \in [1, 3]$. According to the reduction process, g_1, g_2 and g_3 are three rectangle objects in the current window in the cSPOT problem, and $g_i.w = 1$ for $i \in [1, 3]$. Assume that $|W_c| = 1$. The shaded area is the intersection of g_1, g_2 and g_3 . Thus, any point p in the shade area has the maximum burst score, i.e., $S(p) = 3$. The point p in the figure is a bursty point at the given snapshot. The solid line rectangle, whose top-right corner lies in p , is the bursty region as it encloses three spatial objects and its burst score is 3.

In the rest of this section, we present an exact solution to address the cSPOT problem efficiently. Specifically, we first introduce a sweep-line based algorithm, which finds the bursty point given a set of rectangle objects (Section 4.2). Then we present the cell-based lazy update strategy, which determines whether we should invoke the sweep-line algorithm to recompute the bursty point (Section 4.3).

4.2 Detecting Bursty Point on a Snapshot

To address the first challenge, i.e., detecting the bursty point given a snapshot of the stream, we propose a sweep-line based algorithm called SL-cSPOT in this subsection.

The high level idea of the SL-cSPOT algorithm is as follows. We use a horizontal line, referred to as the sweep-line, to scan the space top-down. The sweep-line is divided into $2n + 1$ intervals at most by the vertical edges of the n rectangle objects. For instance, in Fig. 3, the vertical edges of the three rectangles divide the sweep-line into 7 intervals, $\{I_0, \dots, I_6\}$. For each interval I , we use $I.f_c$ and $I.f_p$ to denote the score w.r.t. the current and past windows, respectively for the points on the interval I . We use $I.S$ to denote the burst score of such points. For any interval I_i , the set of rectangles which can cover interval I_i changes when the sweep line meets the top or bottom edge of a rectangle which can cover I_i , and its burst score $I_i.S$ is updated accordingly. A point with the maximum burst score during the sweeping process is returned as the bursty point.

We next illustrate the algorithm with an example. Fig. 3 shows a snapshot of the stream. Rectangle g_1 is in the past window W_p (marked in blue), while g_2 and g_3 are in the current window W_c (marked in red). As shown in Fig. 3, when the sweep-line meets the top edge of g_3 , any point, such as p_1 , which is beneath the overlapped intervals I_3, I_4 and I_5 and above the next horizontal line, will be covered by g_3 . Since g_3 is in the current window, the score of p_1 w.r.t. W_c will be increased by $\frac{g_3.w}{|W_c|} = 2$, resulting in an increase of its burst score. We set $I_i.f_c = 2$ and $I_i.f_p = 0$ for $i \in [3, 5]$, and thus $I_i.S = 0.5 \cdot \max(I_i.f_c - I_i.f_p, 0) + 0.5 \cdot I_i.f_c = 2$ for $i \in [3, 5]$. We select p_1 as the current bursty point. Then the sweep-line meets the top edge of g_1 and g_2 , consecutively. The two edges are processed similarly, and we have $I_4.S = 3$. Thus p_3 is selected as the new bursty point. When the sweep-line meets the bottom edge of the rectangle g_3 , any point, such as p_4 , which is beneath the overlapped intervals and above the next horizontal line, will no longer be covered by g_3 . Thus, the scores w.r.t. W_c of the overlapped intervals I_3, \dots, I_5 are decreased. We have $I_i.f_c = 1$ for $i \in [3, 4]$, and $I_5.f_c = 0$. Their burst scores are updated as: $I_3.S = 1 - \alpha$, $I_4.S = 1$ and $I_5.S = 0$. We repeat this process until the whole space is scanned. Point p_3 has the maximum burst score during the sweeping process. Thus p_3 is returned as the bursty point.

Algorithm 1 outlines this procedure. It takes as input a set of rectangle objects G , and outputs a bursty point p with the maximum burst score in the space. Result point p is initialized as *null*. The algorithm uses a sweep-line to scan the space (lines 2–7). When it meets a horizontal edge of a rectangle r , it first locates the intervals that are covered by r (line 3). Then it updates $I.S$ for each interval I one by one (line 5). The point p is updated if any interval has a larger burst score (lines 6–7).

Algorithm 1. SL-cSPOT Algorithm

Input: A set of rectangle objects G
Output: A bursty point p

- 1: $p = \text{null}$;
- 2: **while** sweep-line meets an horizontal edge of a rectangle g **do**
- 3: $I_i, \dots, I_j \leftarrow$ the intervals covered by g ;
- 4: **for** interval $I \in \{I_i, \dots, I_j\}$ **do**
- 5: Update $I.f_c, I.f_p$ and $I.S$;
- 6: **if** $I.S > S(p)$ **then**
- 7: $p \leftarrow$ a point beneath I , and between the sweep-line and next horizontal edge;
- 8: **return** p ;

Time Complexity. Let n be the number of rectangles. The sweep-line scans $2n$ edges (each rectangle has two horizontal edges). When the sweep-line meets an horizontal edge, $O(2n + 1)$ intervals are affected. So the time complexity is $O(n^2)$.

4.3 Handling the Stream

We have presented Algorithm SL-cSPOT to detect a bursty point given a snapshot of the stream. But how to continuously detect the bursty point? Recall that the burst score of a point is determined by the set of rectangle objects that cover it. The bursty point is likely to change when a rectangle object enters or leaves the sliding windows. Specifically, any of the

following events may change the bursty point: (1) a new rectangle object enters the current window, (2) an existing rectangle object leaves the current window and enters the past window, and (3) an existing rectangle object leaves the past window. We refer to these three events as a *new event*, a *grown event*, and an *expired event*, respectively. We use a tuple $e = \langle g, l \rangle$ to denote an event, where g is the rectangle object, and l is one status from $\{\text{New}, \text{Grown}, \text{Expired}\}$ to indicate the type of the event.

Intuitively, a naïve idea is whenever an event happens, we invoke Algorithm 1 to detect a bursty point on the snapshot of the stream. However, this idea does not address the cSPOT problem efficiently. First, it is not necessary to search the whole space. When an event happens, it only affects the burst score of the points inside the rectangle object of the event. Second, frequent recomputation of the bursty point is computationally expensive. To address the two issues, we next present a cell-based algorithm called *Cell-cSPOT*.

Algorithm 2. Cell-cSPOT Algorithm

Input: An event $e = \langle g, l \rangle$
Output: A bursty point

- 1: $C_g \leftarrow$ cells that are overlapped with g ;
- 2: **for** $c \in C_g$ **do**
- 3: Update $U(c)$ using Eqn (2), (3), and status of $c.p$ using Lemma 4;
- 4: $c \leftarrow \arg \max U(c)$;
- 5: **while** $c.p$ is invalid **do**
- 6: $c.p \leftarrow \text{SL-cSPOT}(c)$;
- 7: $U_d(c) = S(c.p)$;
- 8: $c \leftarrow \arg \max U(c)$;
- 9: **return** $c.p$

4.3.1 Cell-Based Lazy Update

An event only affects the burst scores of the points inside the rectangle of the event. This locality property motivates us to divide the space into *cells*, and develop approaches to handle the cells that are affected by an event. We first define the *grid* that we use as follows.

Definition 6 (Grid and Cell). We consider a grid as a set of vertical and horizontal lines defined by $x = i \cdot b, y = i \cdot a$ for all integers $i \in [-\infty, +\infty]$. For each cell c , we maintain a list of rectangle objects which overlap with the cell over the two sliding time windows W_c and W_p , denoted by $c.G$.

We have the following lemma based on obvious observations.

Lemma 1. A rectangle object of size $a \times b$ overlaps with at most four cells of the grid in Definition 6.

For each cell in the grid, we maintain a burst score upper bound for the points inside the cell (to be discussed in Section 4.3.2). When an event happens, the corresponding rectangle can only affect at most four cells. Instead of searching the affected cells immediately after an event happens, we propose a *lazy update strategy* by utilizing the maintained upper bounds: Whenever an event happens, we first update the upper bounds of the affected cells. Then, we invoke Algorithm 1 to search the cells iteratively in the descending order of their upper bounds. In each iteration, we always

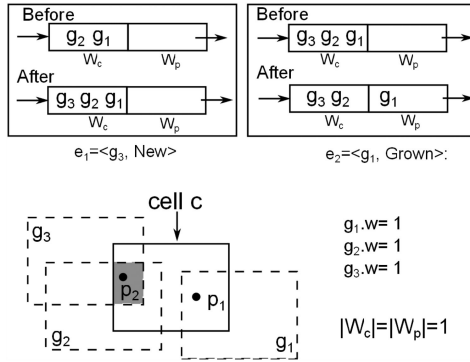


Fig. 4. Cell upper bound.

search the cell with the maximum upper bound. We terminate the process when there is no upper bound larger than the current maximum burst score. Hence, when an event happens, if the upper bounds of the affected cells are less than the current maximum burst score, these cells will not be searched. Thus the lazy update strategy significantly reduces the number of times that Algorithm 1 is invoked to search affected cells.

In addition, to reuse the result of Algorithm 1 from previous iterations, we record the point returned by Algorithm 1 for each cell which is called *candidate point*. The status of each candidate point is either *valid* or *invalid*. If the candidate point of a cell is guaranteed to have the maximum burst score in the cell, its status is *valid*. On the other hand, the status is set to *invalid* if it is unknown whether the candidate point has the maximum burst score. We do not need to invoke Algorithm 1 to search a cell if its candidate point is *valid*. By exploiting the candidate points, we can further avoid searching in some cells (discussed in Section 4.3.3).

Algorithm 2 presents an overview of our algorithm called *Cell-cSPOT* (*cell-based cSPOT*). It takes as input an event $e = \langle g, l \rangle$, and reports a bursty point in the space. The algorithm first locates the set C_g of cells that overlap with g (line 1). Then for each cell c in C_g , it updates its upper bound based on Equations (2), and (3) (to be introduced in Section 4.3.2), and determine the status of the candidate point $c.p$ based on Lemma 4 (to be introduced in Section 4.3.3) (line 3). Then it accesses the cells in descending order of their upper bounds $U(c)$ iteratively (lines 4–8). In each iteration, if the candidate point $c.p$ is *invalid*, we invoke Algorithm 1 to search the cell and update $c.p$ (line 6) and the upper bound (line 7). Otherwise $c.p$ is *valid*, and this indicates that $c.p$ has the maximum burst score in cell c and c has the maximum burst score as there is no cell whose upper bound is larger than the current maximum burst score. Therefore we terminate the process and report point $c.p$ as the result.

Time Complexity. According to Lemma 1, at most four cells are affected by an event rectangle g . Thus, it takes $O(1)$ time to update the upper bounds and candidate points. A cell will not be searched unless it is overlapped with a rectangle object. Thus, $O(1)$ cells are searched in processing a rectangle object. In our implementation, we use a heap to maintain the cells based on their upper bounds. Let $|c_{max}|$ be the maximum number of rectangle objects in a cell. Let n be the number of rectangle objects created in W_c and W_p . It takes $O(\log n)$ time to get the cell c and $O(|c_{max}|^2)$ time to search the cell. Putting these together, the complexity of Algorithm 2 is $O(|c_{max}|^2 + \log n)$.

Space Complexity. Each rectangle object is stored in at most four cells. Thus, the space cost of Algorithm 2 is $O(n)$.

4.3.2 Upper Bound Estimation

Next, we present the details about estimating the upper bound for a cell.

Static Upper Bound. We first consider a simple strategy to estimate an upper bound for a cell. According to the definition of the burst score, rectangle objects in the current window have a positive impact on the burst score, while the rectangle objects in the past window have a non-positive impact. Hence, we can estimate an upper bound burst score for a cell by only utilizing the objects in the current window. We refer to this upper bound as *static upper bound*.

Definition 7 (Static Upper Bound). For a cell c , its static upper bound is computed as follows:

$$U_s(c) = \sum_{g \in c.G \wedge g.t_c \in W_c} \frac{g.w}{|W_c|}, \quad (2)$$

where $c.G$ is a set of rectangle objects overlapped with c .

Lemma 2. For any point p in a cell c , we have $\mathcal{S}(p) \leq U_s(c)$.

Example 4. Consider the example shown in Fig. 4. The solid-line rectangle is a cell in the grid. After event e_1 happens, there are three new rectangle objects overlapped with the cell c . The static upper bound of cell c is $U_s(c) = 3$.

Dynamic Upper Bound. Next, instead of just using objects in the current window, we introduce another way to estimate the upper bound by using both the event and information from the previous computation. Specifically, when an event happens, we dynamically update the upper bound computed from previous upper bound. We refer to such upper bound as *dynamic upper bound*.

Let p_m be the point with the maximum burst score in cell c at a snapshot i when event e_i arrives. Apparently $\mathcal{S}(p_m)$ is an upper bound burst score for cell c at snapshot i . Thus, whenever we search a cell c with Algorithm 1 on a snapshot i , the dynamic upper bound $U_d^i(c)$ can be set as $U_d^i(c) = \mathcal{S}(p_m)$.

Let $U_d^i(c)$ be the upper bound of cell c on snapshot i when event e_i arrives, and $U_d^{i+1}(c)$ be the upper bound when e_{i+1} arrives. Let g be the corresponding rectangle object of e_{i+1} , i.e., $e_{i+1} = \langle g, l \rangle$. Then we have

$$U_d^{i+1}(c) = \begin{cases} U_d^i(c) + \frac{g.w}{|W_c|} & e_{i+1}.l \text{ is New,} \\ U_d^i(c) & e_{i+1}.l \text{ is Grown,} \\ U_d^i(c) + \alpha \frac{g.w}{|W_p|} & e_{i+1}.l \text{ is Expired.} \end{cases} \quad (3)$$

We next show the correctness of the dynamic upper bound with the following lemma.

Lemma 3. Consider a cell c . For any point p in c , we have $\mathcal{S}(p) \leq U_d(c)$ after e happens.

Example 5. Consider the example shown in Fig. 4. We first consider an event $e_1 = \langle g_3, \text{New} \rangle$, i.e., a new rectangle object enters the current window. Assume before e_1 happens, we have searched the cell and the point p_1 has the maximum burst score in c . The dynamic upper bound is set as $U_d^0(c) = 1$. After e_1 happens, we update the dynamic

upper bound as $U_d^1(c) = U_d^0(c) + \frac{g_3.w}{|W_c|} = 2$. Then we consider an event $e_2 = \langle g_1, \text{Grown} \rangle$, i.e., an existing rectangle object g_1 exits the current window and enters the past window. According to Eqn (3), the dynamic upper bound remains the same, i.e., $U_d^2(c) = 2$, since p_2 remains to have the maximum burst score in cell c .

We have presented the static upper bound and the dynamic upper bound. We now combine them for a tighter upper bound.

Definition 8 (Upper bound for cell). For a cell c , we define its upper bound $U(c)$ as $U(c) = \min(U_s(c), U_d(c))$.

4.3.3 Candidate Point Maintenance

An expensive operation of Algorithm 2 is to invoke Algorithm 1 to find a point with the maximum burst score for a cell. To reuse the computation, for each cell c , we maintain a candidate point, denoted by $c.p$, to record the point returned by Algorithm 1. The candidate point has two possible status as introduced in Section 4.3.1. We next present Lemma 4, which is employed to determine the status of a candidate point.

Lemma 4. Let $c.p$ be a point with the maximum burst score in cell c currently. Consider an event $e = \langle g, l \rangle$. After e happens, if either (1) e is either new or expired, g can cover $c.p$, and $f(c.p, W_c) - f(c.p, W_p) > 0$, or (2) e is grown object and g cannot cover $c.p$, then the point $c.p$ still has the maximum burst score.

We determine the status of a candidate point based on Lemma 4. Consider a cell c and an event e which can affect c . If $c.p$ is valid and the conditions in Lemma 4 hold, then $c.p$ remains to be valid. Otherwise, $c.p$ is invalid after e happens.

Example 6. Reconsider the example shown in Fig. 4. We consider the event $e_1 = \langle g_3, \text{New} \rangle$, where a new rectangle g_3 arrives. Before e_1 happens, assume that we have invoked Algorithm 1 to search the cell and p_1 is the point with the maximum burst score. When e_1 happens, since e_1 is new and g_3 cannot cover p_1 , p_1 is invalid after e_1 happens. In fact, points in the shaded area have the maximum burst score after e_1 happens.

5 APPROXIMATE SOLUTIONS

Although our exact solution can continuously detect the bursty region efficiently in real time, we observe that its runtime performance degrades when the number of spatial objects created in time windows W_c and W_p increases significantly (e.g., the sliding windows get larger, the region size gets larger, or the arrival rate of the spatial objects increases). Since a slight imprecision is acceptable in most cases in real life, to tackle this challenge, we propose two algorithms to solve the SURGE problem approximately. We prove that the burst score of the region returned by our proposed approximate algorithms is always bounded by a ratio $\frac{1-\alpha}{4}$ compared to the exact result.

5.1 A Grid-Based Solution

The key idea behind our *grid-based approximate solution* is as follows: We use a grid to divide the space into cells of size $a \times b$. Each cell is a candidate region. By maintaining the

burst score for each cell, we continuously report the cell with the maximum burst score to users as an approximation to the bursty region. A nice feature of this idea is that it is intuitive while it has performance guarantees.

Algorithm 3 outlines our proposed algorithm called GAP-SURGE (Grid-based APProximate SURGE). Here we abuse the notation $e = \langle o, l \rangle$ to denote an event of spatial object o enters or leaves the sliding windows. It first locates the cell that the spatial object o lies in (line 1). The burst score of the cell c is updated accordingly (lines 2–5). The cell with the maximum burst score is returned as an approximate result (line 6).

Algorithm 3. GAP-SURGE Algorithm

```

Input: An event  $e = \langle o, l \rangle$ 
Output: A cell  $c$ 
1:  $c_{i,j} \leftarrow$  the cell  $o$  lies in;
2: if  $e$  is new then  $c_{i,j}.f_c + = \frac{o.w}{|W_c|}$ ;
3: else if  $e$  is grown then  $c_{i,j}.f_c - = \frac{o.w}{|W_c|}$ ,  $c_{i,j}.f_p + = \frac{o.w}{|W_p|}$ ;
4: else  $c_{i,j}.f_p - = \frac{o.w}{|W_c|}$ ;
5:  $c_{i,j}.S = \max(c_{i,j}.f_c - c_{i,j}.f_p, 0) + c_{i,j}.f_c$ ;
6:  $c \leftarrow \arg \max c.S$ ;
7: return  $c$ 
```

Before we show that the region returned by Algorithm 3 has a burst score with an approximation guarantee, we present some interesting properties of the burst score function.

Lemma 5. For any two region r_1 and r_2 , $r_1 \subseteq r_2$, we have $S(r_2) \geq (1 - \alpha)S(r_1)$.

Lemma 6. Let r_1, r_2 be two non-overlapping regions. We have $S(r_1) + S(r_2) \geq S(r_1 \cup r_2)$.

Now we are ready to prove the approximate ratio of Algorithm 3.

Theorem 3. Given a snapshot of the stream, let r be the region returned by Algorithm 3, and r_{opt} be the bursty region returned by our exact solution. We have $S(r) \geq \frac{1-\alpha}{4}S(r_{opt})$.

Lemma 7. The approximation ratio is tight.

Complexity Analysis. In Algorithm 3, it takes constant time to locate the cell and update the burst score. In our implementation, we use a heap to maintain all cells according to their burst scores. Let n be the number of spatial objects created in W_c and W_p . Since there are $O(n)$ non-empty cells, it takes $O(\log n)$ time to report the cell with the maximum burst score.

5.2 A Multi-Grid-Based Solution

The burst score of the region returned by Algorithm 3 is highly dependent on the position of the grid. Inspired by a *grid shifting* technique [20], we propose to invoke Algorithm 3 multiple times with different grids to further improve the result quality.

Note that in the grid shifting [20], they have to carefully choose four grids to guarantee the correctness of the algorithm. However, this is not the case for our multi-grid-based solution. Since Algorithm 3 using a single grid can return a region with bounded quality, we can use any number of grids to invoke Algorithm 3. In this subsection, we use the following four grids as an example to illustrate the algorithm.

$$\begin{aligned} \text{Grid 1: } & x = i \cdot b, y = i \cdot a, \\ \text{Grid 2: } & x = 0.5b + i \cdot b, y = i \cdot a, \\ \text{Grid 3: } & x = b + i \cdot b, y = 0.5a + i \cdot a, \\ \text{Grid 4: } & x = 0.5b + i \cdot b, y = 0.5a + i \cdot a, \end{aligned}$$

for all integers $i \in [-\infty, +\infty]$.

The multi-grid-based solution (called the MGAP-SURGE algorithm) invokes Algorithm 3 four times by using the four different grids. Among the four returned regions, the one with the maximum burst score is returned to users.

Theorem 4. *The approximate ratio of the MGAP-SURGE algorithm is $\frac{1-\alpha}{4}$, i.e., $\mathcal{S}(r) \geq \frac{1-\alpha}{4} \mathcal{S}(r_{opt})$.*

Complexity Analysis. MGAP-SURGE invokes Algorithm 3 four times, and its complexity is $O(\log n)$, where n is the number of spatial objects created in W_c and W_p .

6 TOP-K BURSTY REGION DETECTION

Recall that in Example 1, it is paramount to monitor regions with outbreak of diseases. Intuitively, monitoring only the most bursty region is not sufficient. In fact, it is reasonable to be interested in a small list of such bursty regions. Specifically, given the size of a region, we need to continuously monitor the top- k regions of the given size with highest burst scores. In this section, we present how we can elegantly extend our proposed solutions to continuously detect top- k regions with highest burst scores. We begin by formally defining the *top- k bursty regions*.

6.1 Definition

Although at first glance it may seem that it is easy to define *top- k bursty regions*, in reality it is tricky. First of all, are the top- k regions allowed to overlap? It may seem that detecting k non-overlapping regions is a good choice. However, the non-overlapping requirement may lead us to overlooking some highly bursty regions. Hence, it is beneficial to allow the top- k bursty regions to be overlapping instead of disjoint in nature.

Next, how do we define the burst scores for two overlapped regions? For example, if a spatial object lies at the intersection of two overlapping regions, which region's burst score should it contribute to? A naïve idea is to consider it in both regions. However, this may result in k regions that are highly similar to one another. To resolve this issue, we ensure that a spatial object contributes only to the burst score of at most one region.

The aforementioned considerations lead us to a greedy strategy for defining the *top- k bursty regions*. Specifically, given the first i bursty regions, the $(i+1)$ th bursty region is the region with maximum burst score in the space but excluding all spatial objects that are already covered by the first i bursty regions.

Definition 9 (Top- k Bursty Regions). Consider k rectangular regions r_1, \dots, r_k , each of which has a size of $a \times b$. We say they are the top- k bursty regions if r_i has the maximum burst score over O_i , where O_i is set of objects excluding the objects in $r_1 \cup \dots \cup r_{i-1}$, i.e., $O_i = \{o | o \in O \wedge o \notin r_1 \cup \dots \cup r_{i-1}\}$.

In order to address the top- k bursty regions problem, we reduce the top- k bursty regions problem to k cSPOT problems

following the reduction in Section 4.1. The $(i+1)$ th cSPOT problem aims to detect the $(i+1)$ th bursty point from the space that excludes the set of rectangles that cover the top- i bursty points.

Observe that Definition 9 essentially paves the way to a greedy approach for selecting top- k bursty regions. Whenever an event happens, we can first detect a region with the maximum burst score by invoking Algorithm 1. Then we remove the spatial objects covered by the region. After that, we detect a region with the maximum burst score over the remaining objects. We repeat this process until k regions are selected.

However, the naïve strategy is inefficient as there are too many redundant computations, i.e., it is possible that we search a cell in all the k reduced cSPOT problems. To address the k cSPOT problems efficiently, we want to share the common computations among the k cSPOT problems.

6.2 Extension of the Exact Solution

In the extension of our exact solution, for each cell c , we maintain k upper bounds and k candidate points in order to solve the k cSPOT problems by following the idea of Algorithm 2. For each cSPOT problem, we adopt the lazy update strategy to access the cells in descending order of their upper bounds. If the candidate point of the top cell is not valid, we search the cell by invoking Algorithm 1.

We develop two ideas of sharing the computations among the k cSPOT problems. First, if a rectangle object can cover the i th bursty point, it will not be considered in the cSPOT problems with order higher than i . For the extension, we maintain a level, denoted by $g.lvl$, for each rectangle object g . To select the i th bursty point in response to a new event, we consider the set of rectangles $G[i : k]$ whose levels are no smaller than i , i.e., $G[i : k] = \{g | g.lvl \geq i\}$. When the i th bursty point is selected, the levels of all the rectangles that cover the i th bursty point are set as i , and these rectangles will not be considered by the cSPOT problems with a higher order than i . Meanwhile, if a rectangle covers the old i th bursty point, but not the new i th point, its level is reset to k so that it will be considered in all the k cSPOT problems.

Second, if no rectangle in a cell covers any of the k detected bursty points, all the rectangles in the cell will be considered in all k cSPOT problems. Thus, the upper bounds and the candidate points w.r.t. the k cSPOT problems for the cell are the same. That is, once the upper bound and the candidate point for the cell are computed for one cSPOT problem, we do not need to recompute them again for other cSPOT problems.

Algorithm 4 presents the detail of our extension. It takes as input an event $e = \langle g, l \rangle$, and outputs the top- k bursty points, denoted by $p[1 : k]$. It uses V to denote the set of objects that need to be handled subsequently, and is initialized as $\{g\}$ (line 1). It then solves the k cSPOT problem iteratively (lines 2–17). In each cSPOT problem, it first locates the set of cells affected by the objects in V (line 4). For each cell $c \in C$, the upper bound $U(c)[j]$ and candidate point $c.p[j]$ w.r.t. the j th cSPOT problem are updated for $j \in [i, k]$ (lines 5–6). Then it accesses the cells in descending order of their upper bounds w.r.t. the i th cSPOT problem (lines 8–14). The upper bound and candidate point are updated as in Algorithm 2 (lines 9–10). If no rectangle in cell c covers any of the k detected bursty points, its k upper bounds and candidate

TABLE 1
Datasets

Datasets	UK	US	Taxi
# of Spatial Objects	1,000,000	1,000,000	1,000,000
Arrival Rate(per hour)	5,747	16,802	18,145
Range of Latitude	139.0 150.9	100.1 150.4	41.6 42.2
Range of Longitude	171.1 181.9	40.2 118.8	12.0 12.9

points are set to the same (lines 11-12). When a new bursty point is found, we reset the levels for the affected objects as discussed earlier (lines 15–16): The rectangles that cover the old bursty point p_{old} but not the new bursty point $p[i]$ are newly visible to all the k cSPOT problems, while the rectangles that cover the new bursty point $p[i]$ are newly invisible to the cSPOT problems with a higher order than i . The two types of rectangle objects comprise V , which will be processed in the next cSPOT problem (line 17). After k iterations, it returns the top- k bursty points $p[1 : k]$ as the result.

Algorithm 4. ccs-KSURGE Algorithm

```

Input: An event  $e = \langle g, l \rangle$ 
Output: A bursty point
1:  $g.lvl = k, V = \{g\};$ 
2: for  $i \in [1, k]$  do
3:    $p_{old} = p[i];$ 
4:    $C \leftarrow$  cells that are overlapped with  $V$ ;
5:   for  $c \in C$  do
6:     Update  $U(c)[j]$  and  $c.p[j]$  for  $j \in [i, k]$ ;
7:    $c \leftarrow \arg \max U(c)[i];$ 
8:   while  $c.p[i]$  is invalid do
9:      $c.p[i] \leftarrow$  SL-cSPOT( $c$ ) over  $G[i :];$ 
10:     $U_d(c)[i] = \mathcal{S}(c.p[i])$  over  $G[i :];$ 
11:    if no rectangle in  $c$  covers any of  $p[1 : k]$  then
12:       $c.p[1 : k] = c.p[i], U_d(c)[1 : k] = U_d(c)[i];$ 
13:       $c \leftarrow \arg \max U(c)[i];$ 
14:     $p[i] \leftarrow c.p;$ 
15:    Mark  $o.lvl = k$  for any  $o \in G(p_{old})[i] \setminus G(p[i])[i : k];$ 
16:    Mark  $o.lvl = i$  for any  $o \in G(p[i])[i : k];$ 
17:     $V \leftarrow G(p[i])[i : k] \cup G(p_{old})[i];$ 
18: return  $p[1 : k]$ 

```

Complexity Analysis. A cell is searched if its upper bound is either changed by an event or by a detected bursty point. Thus, the algorithm searches $O(1 + k) = O(k)$ cells on average when processing a rectangle. The complexity of Algorithm 4 is $O(|c_{max}|^2 \cdot k)$, where $|c_{max}|$ is the maximum number of objects that we search in a cell.

6.3 Extension of the Approximate Solutions

We also extend our approximate solutions in Section 5 to find k regions with relatively high burst score.

Extending the GAP-SURGE Algorithm. Consider the grid-based solution. We use a heap to maintain all cells with their burst scores. Thus, we can simply return top- k cells with highest burst scores. In our implementation, we use a heap to maintain the cells. Thus, its complexity is $O(\log n)$.

Extending the mGAP-SURGE Algorithm. We extend the multi-grid-based solution similarly. Note that one cell in a grid may overlap with at most four cells in another grid. Thus, for each grid, we maintain the top- $4k$ cells. Then we merge

the $16 \cdot k$ cells and return the top- k non-overlapping cells. Its time complexity is $O(\log n + k)$.

7 EXPERIMENTAL STUDY

We investigate the performance of our proposed techniques. All algorithms are implemented in C++ complied with GCC 4.8.2. The experiments are conducted on a machine with a 2.70 GHz CPU and 64 GB of memory running Ubuntu.

7.1 Experimental Setup

Datasets. We conduct experiments on three public real-life datasets as reported in Table 1. UK consists of 1,000,000 geo-tagged tweets posted in UK. US consists of 1,000,000 geo-tagged tweets posted in US and has a higher arrival rate. Taxi⁴ consists of mobility traces of taxi cabs obtained from the GPS in Roma, Italy. It contains 1,000,000 records over 5 days. For each dataset, the weight of each spatial object is randomly chosen from [1, 100] with a uniform distribution.

Algorithms. We evaluate the performances of the three proposed algorithms, namely the exact method *Cell-cSPOT* (denoted by CCS), the grid-based approximation algorithm *GAP-SURGE* (denoted by GAPS), and the multi-grid-based technique *mGAP-SURGE* (denoted by MGAPS). We denote the top- k extensions of these algorithms as kCCS, kGAPS, and kMGAPS, respectively. To evaluate the usefulness of our proposed method of upper bound estimation, we compare CCS with an approach that only utilizes the static upper bound. We denote this baseline method by B-CCS. We also compare CCS with a baseline approach that does not use any upper bound estimation technique, denoted by Base. Specifically, in Base we divide the space into cells, and we search all the cells that overlap with the rectangle object when an event happens. To the best of our knowledge, there is no existing technique that addresses the SURGE problem. Hence we are confined to compare our proposed algorithms with aG2 [1], which is designed for continuously monitoring the MaxRS problem. Obviously, we cannot directly apply it to solve the SURGE problem. In our experiments, we use a modified version of aG2. Specifically, the modified algorithm inherits the grid index structure and the branch-and-bound strategy from the original algorithm. The main difference between the modified and the original algorithms is how we search a rectangle object given a snapshot of the stream. In the original algorithm, they invoke the sweep-line algorithm [18] to search a rectangle object to find a region with maximum sum score, while in the modified algorithm, we use our proposed SL-cSPOT algorithm instead.

Parameters. By default, we set the size of the past window W_p and the current window W_c as 1 hour for US and UK, and 5 minutes for Taxi. We set the size of the query rectangle as 1/1000 of the range of each dataset by default, denoted by q . We set the preferred area A as the whole space. For the aG2 algorithm, we set the size of a cell to $10q$.

Stream Workload. We start the simulation when the system becomes stable, i.e., there exists an expired object from the past sliding window. We continuously run each algorithm for 1,000,000 new arriving spatial objects over the two sliding windows. The average processing time per object is reported.

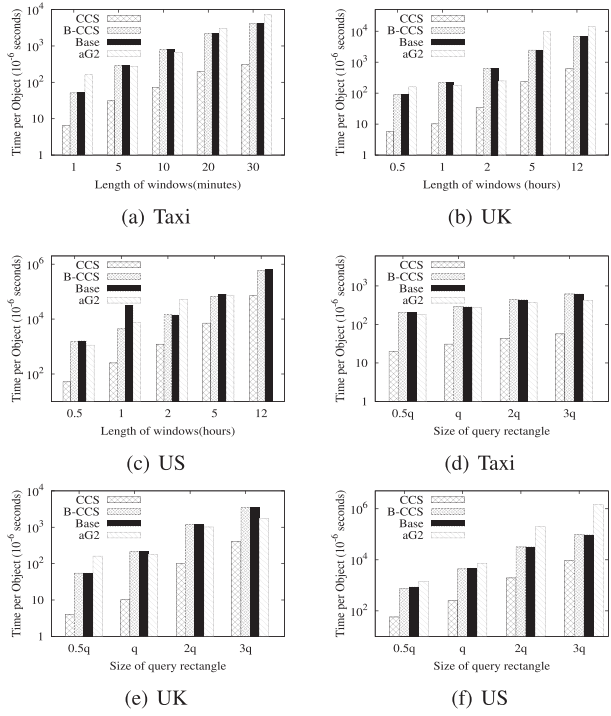


Fig. 5. Runtime of CCS, B – CCS, Base, and aG2.

7.2 Evaluation of the Exact Solution

We first evaluate the runtime performance of CCS, B-CCS and Base on each dataset. Then we study the usefulness of the upper bound in CCS.

Runtime Performance. The aim of the first set of experiments is to evaluate the efficiency of our exact solution *w.r.t.* the sliding window size and the query rectangle size. For US and UK, we vary the sliding window with the following sizes: 30 minutes, 1 hour, 2 hours, 5 hours, and 12 hours. For Taxi, we use the following five sizes for sliding windows: 1 minute, 5 minutes, 10 minutes, 20 minutes, and 30 minutes. We use the following four sizes for the query rectangle: $0.5q$, q , $2q$, and $3q$.

Figs. 5a, 5b, and 5c report the average runtime of the three methods for processing one spatial object as we vary the size of sliding windows. Note that the *y*-axis is in logarithmic scale. We find that CCS runs efficiently and outperforms aG2. For example, for Taxi, it takes about 3×10^{-4} seconds to process an object when the current and past windows are both set to 30 minutes, while aG2 takes 7×10^{-3} seconds. In addition, we find that aG2 runs out of the 64 GB memory on US when the current window and past window are both set as 12 hours, as there are too many spatial objects in the two sliding windows.

Moreover, we observe that the processing time per object of all algorithms increases as the size of window increases. This is due to the need to consider a larger number of spatial objects when we search for the bursty region with the increase in size of the sliding window. Consequently, the runtime per object increases.

Figs. 5d, 5e, and 5f report the average runtime for processing one spatial object as we vary the size of the query rectangle. Similarly, the average runtime increases as size of the rectangle increases.

Usefulness of Upper Bound. Next, we evaluate the usefulness of the method for upper bound estimation in CCS. In

TABLE 2
Ratio of Rectangle Messages that Trigger a Search versus Window Size for CCS and B-CCS

Taxi	Window (mins)	1	5	10	20	30
		CCS	4.85%	3.20%	2.56%	2.13%
		B-CCS	92.63%	78.30%	70.00%	57.90%
UK	Window (hours)	0.5	1	2	5	12
		CCS	0.34%	0.27%	0.23%	0.37%
		B-CCS	37.79%	28.23%	22.76%	21.64%
US	Window (hours)	0.5	1	2	5	12
		CCS	0.60%	0.68%	0.70%	0.52%
		B-CCS	64.21%	52.29%	35.13%	9.0%

TABLE 3
Approximate Ratio versus the Size of Window

Taxi	Window (mins)	1	5	10	20	30	
		GAPS	76.34%	73.90%	75.12%	75.70%	76.35%
		MGAPS	85.98%	85.14%	87.35%	88.34%	87.85%
UK	Window (hours)	0.5	1	2	12	24	
		GAPS	90.22%	91.56%	91.98%	89.82%	92.44%
		MGAPS	93.13%	94.34%	93.76%	90.50%	92.82%
US	Window (hours)	0.5	1	2	12	24	
		GAPS	84.23%	80.67%	89.70%	91.77%	80.10%
		MGAPS	88.61%	88.07%	91.44%	91.77%	84.34%

this set of experiments, we process 1,000,000 new objects and report how many rectangles trigger a search. The results are reported in Table 2. Clearly, only a small portion of rectangle messages (2-5 percent for Taxi, and less than 1 percent for US and UK) trigger a search in CCS compared with B-CCS. This is because CCS can estimate a much tighter upper bound for cells. Thus, many cells are eliminated from further checking. This also explains why CCS is much more efficient than B-CCS. As shown in Fig. 5, we observe that CCS is more efficient than the other two methods. The runtime of CCS is more than one order of magnitude faster than B-CCS and Base, respectively. Moreover, we observe that B-CCS is only marginally better than BASE, which indicates that only using the static upper bound cannot effectively avoid unnecessary recomputation. This is because the static upper bound is too loose, especially when the weights of the objects are randomly chosen from 1 to 100.

7.3 Evaluation of the Approximate Solutions

Approximate Ratio. In this set of experiments, we vary the sliding window to assess the approximate ratio of the burst scores of region detected by GAPS and MGAPS. The detailed results are reported in Table 3. Though the theoretical approximate ratio is $\frac{1-\alpha}{4}$, in practice it is much better, especially for MGAPS. We observe that for UK, the burst score of the region detected by GAPS is about 70–90 percent of the burst score of the optimal region. The region detected by MGAPS is about 85–95 percent of the burst score of the optimal region. Since GAPS and MGAPS are much more efficient than CCS (about three orders of magnitude faster), they are good alternatives to CCS when a slight imprecision is acceptable.

Runtime Performance. We evaluate the efficiency of our approximate solutions *w.r.t.* the sliding window size and the query rectangle size under the same setting as for the exact

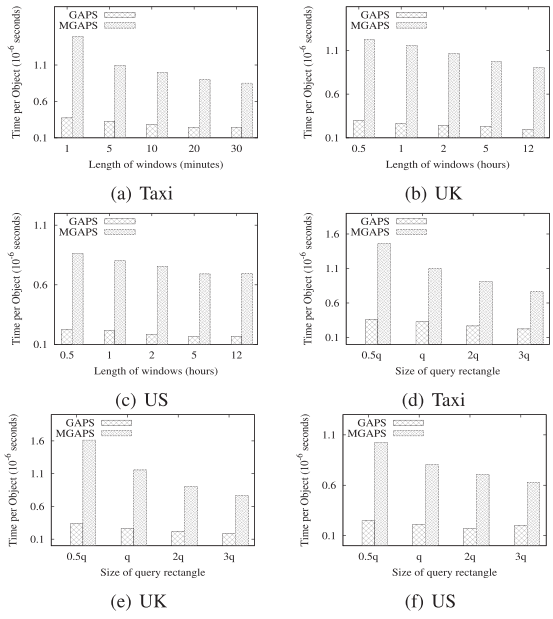
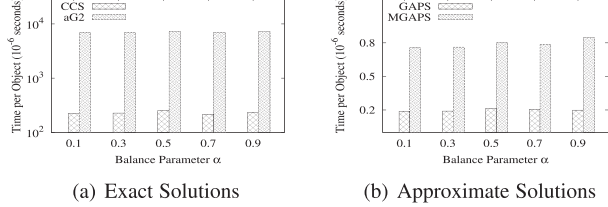


Fig. 6. Runtime performance of GAPS and MGAPS.

Fig. 7. Runtime performance w.r.t. α on US.

solution. Figs. 6a, 6b, and 6c report the average runtime for processing one spatial object using GAPS and MGAPS as we vary the sliding window. Figs. 6d, 6e, and 6f report the average runtime for processing one spatial object as we vary the size of the query rectangle. We find that the runtime of MGAPS is about 2-5 times of GAPS, which is expected as MGAPS invokes GAPS four times. Moreover, GAPS and MGAPS are about three orders of magnitude faster than CCS by comparing Figs. 5 and 6.

7.4 Effect of α

In the definition of burst score, we use a parameter α to balance the significance and the burstiness. In this set of experiments, we evaluate the impact of the parameter α on the efficiency and approximation ratio of our proposed algorithms on the US dataset. We use 1 hour for the sliding windows and q for the size of the query rectangle.

Impact on Runtime Performance. We evaluate the efficiency of our exact and approximate solutions w.r.t. the balance parameter α . Fig. 7 reports the average runtime for processing one spatial object as we vary α from 0.1 to 0.9. We observe that the efficiency is hardly affected by the parameter α for both our exact solution and approximate solutions.

Impact on Approximation Ratio. In this set of experiments, we evaluate the approximate ratio of the burst scores of regions detected by GAPS and MGAPS by varying α . The results are reported in Table 4. We find that the approximate ratios of the two algorithms decrease as α increases. This is because their theoretical approximate ratio $\frac{1-\alpha}{4}$ decreases as α increases.

TABLE 4
Approximate Ratio versus α

US	α	GAPS	0.1	0.3	0.5	0.7	0.9
		MGAPS	90.50%	89.44% ^b	88.07%	87.80%	86.67%

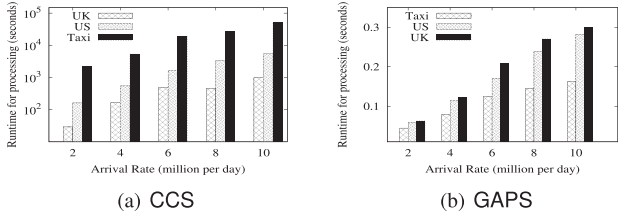


Fig. 8. Scalability study.

7.5 Scalability

We now investigate the scalability of our proposed techniques by varying the arrival rate of the spatial objects. Specifically, we use 1 hour for both the current window and past window, and q for the size of the query rectangle on all three datasets. We stretch the stream to change its arrival rate from 2 million per day to 10 million per day. For example, in UK, 1 million spatial objects arrived in 174 hours. Hence, we shrink the arrival time of each object to make all objects arrive in 24 hours. Then the arrival rate of the stream is 1 millions per day. We only report the *average time* for processing the objects arrived in one hour (denoted by t_h) of CCS and GAPS in Fig. 8. Formally, $t_h = \frac{\text{runtime}}{|\mathcal{O}|_{\text{time}}}$, where *runtime* is the runtime of the algorithm, and $|\mathcal{O}|_{\text{time}}$ is the total timespan of the stream.

We observe that it takes several hours for CCS to process the objects arrived in an hour for the Taxi dataset, which means that it does not scale well and cannot handle streams with high arriving rate. On the other hand, our approximate solutions, GAPS and MGAPS, scale well with the increase in arrival rate. They can process the objects arrived in an hour within seconds.

Note that the complexity of CCS is determined by the maximum number of objects in a cell, while the GAPS is determined by the number of non-empty cells. In Taxi, the objects in W_c and W_p are likely to be located close to each other. Thus, there are fewer non-empty cells and each cell is likely to have many objects. As a result, we can observe that CCS has the worst efficiency in Taxi datasets, while GAPS has the best efficiency in Taxi datasets in Fig. 8.

7.6 Finding Top-k Bursty Regions

We next evaluate the performance of the extensions of our three algorithms for continuously detecting top- k bursty regions. We study the effect of k and the size of sliding windows.

Runtime Performance. This set of experiments aims to evaluate the efficiency of these algorithms w.r.t. the sliding window size. We adopt the same setting as in Section 7.2. Figs. 9a, 9b, and 9c report the average runtime per object of kCCS, kGAPS, and kMGAPS for different sliding windows. We observe that as the sliding window gets larger, kCCS does not scale well and cannot process the top- k queries efficiently. Meanwhile, kGAPS and kMGAPS can find top- k bursty regions efficiently.

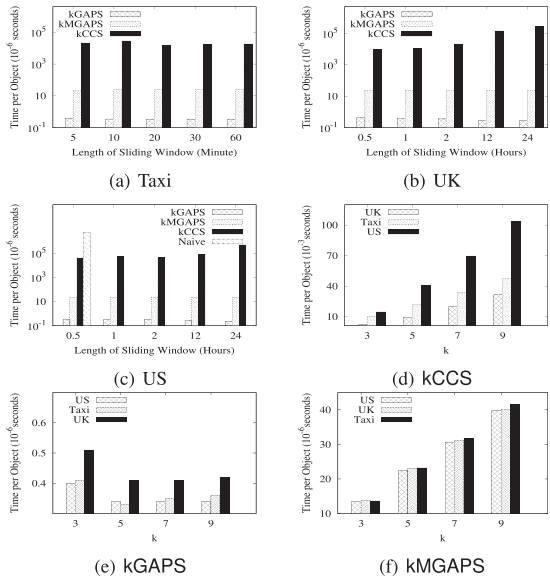
Fig. 9. Top- k bursty regions detection.

Fig. 10. Bursty region about “concert”.

We also compare the naïve solution for finding top- k bursty regions with these algorithms. Recall from Section 6, in the naïve solution, we detect the top- k bursty regions for each newly-arrived object. Clearly, the naïve solution is prohibitively expensive. Hence, we only run it with a small sliding window on US, and its runtime per object is about 100X more than kCCS.

Effect of k . Next, we study how the value of k affect the runtime performance of the three extensions. We use the following 4 values for k : 3, 5, 7 and 9. The runtime performance is depicted in Figs. 9d, 9e, and 9f. We observe the runtime per object of kCCS increases as k increases. This is because we divide the top- k bursty region detection problem into k instances of bursty region detection problems. Each bursty region detection problem takes $O(n_c^2)$ time to find a bursty region, where n_c is the number of spatial objects in the cells that we actually searched. We also observe that kGAPS and kMGAPS are less affected by k .

7.7 Case Study

Example of Bursty Region. We first conduct a case study to show the region monitored by *cell-cSPOT*. We run the *cell-cSPOT* algorithm on the tweets containing keyword “concert” posted in United States from 2012 April to 2012 October. Note that since the algorithm continuously reports the location of bursty regions, we only present one example of the detected bursty region and explain the connection between the region and the real life event.

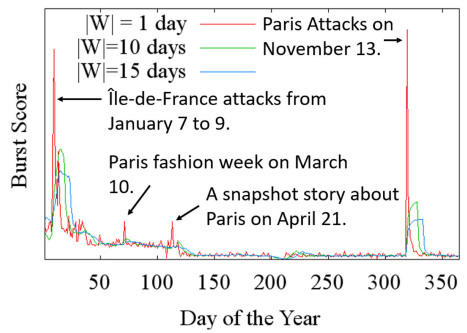


Fig. 11. Burst score of the U.S. in 2015.

On July 8, 2012, our algorithm detected a region as shown in Fig. 10. The frequent keywords in this region during this time are “Walt” and “Concert”. This is because a concert was performed by Katherine Eason with Inner City Youth Orchestra of Los Angeles in Walt Disney Concert Hall in the detected region on that day.

Effect of Window Size. We next conduct a case study to shed some light on the selection of $|W|$. Specifically, we consider a fixed region which can cover the U.S., and report how the burst score of the region changes along with time. We use the following three sliding windows: 1 day, 10 days and 15 days. We consider the tweets containing keyword “Paris” posted in 2015. The result is reported in Fig. 11.

We observe that when we vary the size of the sliding windows, we can capture bursts in different granularities. Specifically, we notice that when the sliding window is large, only big bursts (e.g., the terrorist attacks in Paris.) can be captured. Moreover, we notice that the burst score using a small sliding window is capable to capture a small surge in tweets when less significant events happen (e.g., famous actors made appearance in a fashion show, or a video about Paris became a trend topic.).

In summary, the size of the sliding window determines the granularity of the detected bursts. A small sliding window is capable to detect a small burst. However, due to the large number of small bursts in real life, the location of the bursty region could be updated frequently, leading to a less meaningful bursty region occasionally. User should select the proper sliding window based on the application. In most cases, 1 hour or 1 day are good enough to provide meaningful results.

8 CONCLUSIONS

The work reported in this paper is motivated by new opportunities brought by the massive volumes of streaming geotagged data (i.e., spatial objects) generated by location-enabled mobile devices. Specifically, we have studied a new problem called the SURGE problem to continuously detect the bursty region in a given area in real time. The SURGE problem is important as it can underpin various applications such as disease outbreak detection. We have proposed an exact solution and two approximate solutions for SURGE. We have also extended these solutions to find top- k bursty regions. Finally, our experiment study with real-world datasets has demonstrated the efficiency of our framework. As part of future work, we intend to explore the SURGE problem in the context of road network.

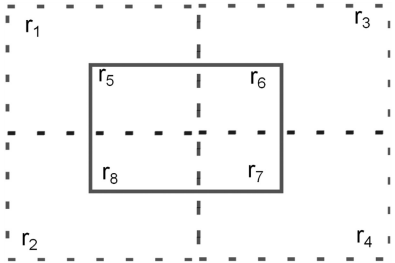


Fig. 12. Proof for Theorem 3.

APPENDIX PROOFS

Proof for Theorem 1. Let p be any point in the cSPOT problem, and r be the rectangular region of size $a \times b$ whose top-right corner is located at p . A spatial object o is in r iff the corresponding rectangle object g can cover p . Since the corresponding o and g have the same creation time and weight, we can derive that $f(r, W_c) = f(p, W_c)$, $f(r, W_p) = f(p, W_p)$, and thus r and p have the same burst score. As a result, if the point p_m has the maximum burst score in the cSPOT problem, then r_m also has the maximum burst score in the SURGE problem.

Proof for Lemma 2. We have

$$\begin{aligned} S(p) &= \alpha \max(f(p, W_c) - f(p, W_p), 0) + (1 - \alpha)f(p, W_c) \\ &\leq \alpha f(p, W_c) + (1 - \alpha)f(p, W_c) = f(p, W_c) = U_s(c). \end{aligned}$$

Proof for Lemma 3. Let $\Delta S(p)$, $\Delta f(p, W)$ be the increase of $S(p)$ and $f(p, W)$ after e happens, respectively. We assume that no two events arrive at the same time. We discuss the following three cases.

Case 1: e is New. For any point p that is covered by g , its current score is increased by $\Delta f(p, W_c) = \frac{g \cdot w}{|W_c|}$. We have $\Delta S(p) \leq \Delta f(p, W_c) = \frac{g \cdot w}{|W_c|}$.

Case 2: e is Grown. For any point p that is covered by g , its current score is decreased, i.e., $\Delta f(p, W_c) = -\frac{g \cdot w}{|W_c|}$ and its past score is increased, i.e., $\Delta f(p, W_p) = \frac{g \cdot w}{|W_p|}$. Thus, we can easily get $\Delta S(p) \leq 0$.

Case 3: e is Expired. For any point p covered by g , its current score is not affected, and its past score is decreased, i.e., $\Delta f(p, W_p) = -\frac{g \cdot w}{|W_p|}$. Thus, we have $\Delta S(p) \leq \alpha(-\Delta f(p, W_p)) = \alpha \frac{g \cdot w}{|W_p|}$.

Since $\Delta S(p) \leq \Delta U_d(c)$, we still have $S(p) \leq U_d(c)$.

Proof for Lemma 4. We use Δ to denote the increase of the score. We consider the following three cases.

Case 1: $e.l$ is New. We have $\Delta S(c.p) = \frac{g \cdot w}{|W_c|}$ if and only if g can cover $c.p$ and $f(c.p, W_c) - f(c.p, W_p) > 0$. In this case, $c.p$ still has the maximum burst score as $\Delta S(p) \leq \frac{g \cdot w}{|W_c|}$ for any p in g (Lemma 3). Otherwise, it is possible that there exists a point p' in g with a larger increase such that p' has a larger burst score than $c.p$ after g arrives.

Case 2: $e.l$ is Grown. For any point p in g , the increase $\Delta S(p) < 0$. If g does not cover $c.p$, $c.p$'s burst score does not change and it still has the maximum burst score. Otherwise, $c.p$'s burst score is decreased and could be exceeded by a point outside g .

Case 3: $e.l$ is Expired. As shown in the proof for Lemma 3, $\Delta S(p) \leq \alpha \frac{g \cdot w}{|W_c|}$ for any p in g . We have $\Delta S(c.p) = \alpha \frac{g \cdot w}{|W_c|}$ if and

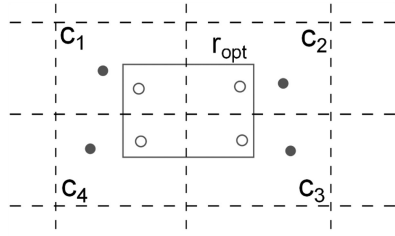


Fig. 13. A tight example.

only if g can cover $c.p$ and $f(c.p, W_c) - f(c.p, W_p) > 0$. In this case, $c.p$ still has the maximum burst score. Otherwise, similar to Case 1, it is possible that there exists a point p' in g with a larger increase of burst score.

Putting these together, the lemma is proved.

Proof for Lemma 5. According to the definition of the burst score, we have

$$\begin{aligned} S(r_2) &= \alpha \max(f(r_2, W_c) - f(r_2, W_p), 0) + (1 - \alpha)f(r_2, W_c) \\ &\geq (1 - \alpha)f(r_2, W_c) \geq (1 - \alpha)f(r_1, W_c) \geq (1 - \alpha)S(r_1). \end{aligned}$$

Proof for Lemma 6. Since r_1 and r_2 are non-overlapping, according to the definition of burst score, we have $f(r_1, W) + f(r_2, W) = f(r_1 \cup r_2, W)$ for either $W \in \{W_c, W_p\}$. Then we can easily get

$$\begin{aligned} &\max(f(r_1 \cup r_2, W_c) - f(r_1 \cup r_2, W_p), 0) \\ &\leq \max(f(r_1, W_c) - f(r_1, W_p), 0) \\ &\quad + \max(f(r_2, W_c) - f(r_2, W_p), 0). \end{aligned}$$

Thus, we have $S(r_1 \cup r_2) \leq S(r_1) + S(r_2)$.

Proof for Theorem 3. Since the sizes of r_{opt} and any cell are both $a \times b$, then r_{opt} either overlaps with a cell or intersects with four cells. We consider the following two cases.

Case 1: r_{opt} Overlaps One Cell. Since we return the candidate with maximum burst score, we will return the bursty region to users. The approximate ratio is 1.

Case 2: r_{opt} Intersects with 4 Cells. Consider the example shown in Fig. 12. Let the solid line rectangle be r_{opt} . The four dashed line rectangles are four cells which intersect with r_{opt} . According to Lemma 5, we have $(1 - \alpha)S(r_{opt}) \leq S(c_1 \cup \dots \cup c_4)$. According to Lemma 6, we can derive that $S(c_1 \cup \dots \cup c_4) \leq \sum_{i \in [1, 4]} S(c_i)$. Since we report the cell with the maximum burst score, i.e., $S(r) \geq S(c_i)$ for any $i \in [1, 4]$. Thus, we have $\frac{1-\alpha}{4}S(r_{opt}) \leq S(r)$.

Proof for Lemma 7. We show the approximation ratio is tight by giving an example. Consider an instance in Fig. 13, where c_1, c_2, c_3 and c_4 are cells in the grid, and the solid-line rectangle r_{opt} is the bursty region with the maximum burst score. The white nodes are the spatial objects in window W_c and the black nodes are in W_p . We assume that $\frac{o.w}{|W_c|} = \frac{o.w}{|W_p|} = 1$ for each object o . The burst score for the region r_{opt} is $S(r_{opt}) = \alpha \max(4 - 0, 0) + (1 - \alpha)4 = 4$. The burst score of cell c_i is $S(c_i) = \alpha \max(1 - 1, 0) + (1 - \alpha) = 1 - \alpha$, for any $i \in [1, 4]$. Thus, the approximation ratio is tight.

Proof for Theorem 4. Since the mGAP-SURGE returns the best result of found by Algorithm 3, its approximation ratio is $\frac{1-\alpha}{4}$.

ACKNOWLEDGMENTS

This work is supported in part by National Key R&D Program of China 2018YFB1700403, and NSFC U1636210&61421003. This research is supported by a MOE Tier-2 grant MOE2016-T2-1-137, and a MOE Tier-1 grant RG31/17. The authors also would like to thank the anonymous reviewers for their valuable comments.

REFERENCES

- [1] D. Amagata and T. Hara, "Monitoring MaxRS in spatial data streams," in *Proc. Int. Conf. Extending Database Technol.*, 2016, pp. 317–328.
- [2] A. Bulut and A. K. Singh, "A unified framework for monitoring data streams in real time," in *Proc. Int. Conf. Data Eng.*, 2005, pp. 44–55.
- [3] X. Cao, G. Cong, C. S. Jensen, and M. L. Yiu, "Retrieving regions of interest for user exploration," *Proc. VLDB Endowment*, vol. 7, no. 9, pp. 733–744, 2014.
- [4] L. Chen, G. Cong, and X. Cao, "An efficient query indexing mechanism for filtering geo-textual data," in *Proc. ACM SIGMOD Int. Conf. Manage. Data*, 2013, pp. 749–760.
- [5] L. Chen, G. Cong, X. Cao, and K.-L. Tan, "Temporal spatial-keyword top-k publish/subscribe," in *Proc. Int. Conf. Data Eng.*, 2015, pp. 255–266.
- [6] D.-W. Choi, C.-W. Chung, and Y. Tao, "A scalable algorithm for maximizing range sum in spatial databases," *Proc. VLDB Endowment*, vol. 5, no. 11, pp. 1088–1099, 2012.
- [7] K. Feng, G. Cong, S. S. Bhowmick, W.-C. Peng, and C. Miao, "Towards best region search for data exploration," in *Proc. Int. Conf. Manage. Data*, 2016, pp. 1055–1070.
- [8] K. Feng, T. Guo, S. S. Cong, G. Bhowmick, and S. Ma, "SURGE: Continuous detection of bursty regions over a stream of spatial objects," in *Proc. 34th Int. Conf. Data Eng.*, 2018, pp. 1292–1295.
- [9] G. P. C. Fung, J. X. Yu, P. S. Yu, and H. Lu, "Parameter free bursty events detection in text streams," in *Proc. 1st Int. Conf. Very Large Data Bases*, 2005, pp. 181–192.
- [10] H. Hu, Y. Liu, G. Li, J. Feng, and K.-L. Tan, "A location-aware publish/subscribe framework for parameterized spatio-textual subscriptions," in *Proc. Int. Conf. Data Eng.*, 2015, pp. 711–722.
- [11] M. M.-U. Hussain, G. Trajcevski, K. A. Islam, and M. E. Ali, "Towards efficient maintenance of continuous MaxRS query for trajectories," in *Proc. 20th Int. Conf. Extending Database Technol.*, 2017, pp. 402–413.
- [12] C. S. Jensen, D. Lin, B. C. Ooi, and R. Zhang, "Effective density queries on continuously moving objects," in *Proc. Int. Conf. Data Eng.*, 2006, pp. 71–71.
- [13] J. Kleinberg, "Bursty and hierarchical structure in streams," *Data Mining Knowl. Discovery*, vol. 7, no. 4, pp. 373–397, 2003.
- [14] T. Lappas, M. R. Vieira, D. Gunopulos, and V. J. Tsotras, "On the spatiotemporal burstiness of terms," *Proc. VLDB Endowment*, vol. 5, no. 9, pp. 836–847, 2012.
- [15] G. Li, Y. Wang, T. Wang, and J. Feng, "Location-aware publish/subscribe," in *Proc. 19th ACM SIGKDD Int. Conf. Knowl. Discovery Data Mining*, 2013, pp. 802–810.
- [16] J. Liu, G. Yu, and H. Sun, "Subject-oriented top-k hot region queries in spatial dataset," in *Proc. Conf. Inf. Knowl. Manage.*, 2011, pp. 2409–2412.
- [17] M. Mathioudakis, N. Bansal, and N. Koudas, "Identifying, attributing and describing spatial bursts," *Proc. VLDB Endowment*, vol. 3, no. 1/2, pp. 1091–1102, 2010.
- [18] S. C. Nandy and B. B. Bhattacharya, "A unified algorithm for finding maximum and minimum object enclosing rectangles and cuboids," *Comput. Math. Appl.*, vol. 29, no. 8, pp. 45–61, 1995.
- [19] J. Ni and C. V. Ravishankar, "Pointwise-dense region queries in spatio-temporal databases," in *Proc. Int. Conf. Data Eng.*, 2007, pp. 1066–1075.
- [20] Y. Tao, X. Hu, D.-W. Choi, and C.-W. Chung, "Approximate MaxRS in spatial databases," *Proc. VLDB Endowment*, vol. 6, no. 13, pp. 1546–1557, 2013.
- [21] X. Wang, C. Zhai, X. Hu, and R. Sproat, "Mining correlated bursty topic patterns from coordinated text streams," in *Proc. 13th ACM SIGKDD Int. Conf. Knowl. Discovery Data Mining*, 2007, pp. 784–793.
- [22] X. Wang, Y. Zhang, W. Zhang, X. Lin, and Z. Huang, "Skype: Top-k spatial-keyword publish/subscribe over sliding window," *Proc. VLDB Endowment*, vol. 9, no. 7, pp. 588–599, 2016.
- [23] X. Wang, Y. Zhang, W. Zhang, X. Lin, and W. Wang, "Selectivity estimation on streaming spatio-textual data using local correlations," *Proc. VLDB Endowment*, vol. 8, no. 2, pp. 101–112, 2014.
- [24] X. Wang, Y. Zhang, W. Zhang, X. Lin, and W. Wang, "AP-Tree: Efficiently support continuous spatial-keyword queries over stream," in *Proc. IEEE 31st Int. Conf. Data Eng.*, 2015, pp. 1107–1118.
- [25] C. Zhang, G. Zhou, Q. Yuan, H. Zhuang, Y. Zheng, L. M. Kaplan, S. Wang, and J. Han, "GeoBurst: Real-time local event detection in geo-tagged tweet streams," in *Proc. Int. Conf. Res. Develop. Inf. Retrieval*, 2016, pp. 513–522.
- [26] Y. Zhu and D. Shasha, "Efficient elastic burst detection in data streams," in *Proc. 9th ACM SIGKDD Int. Conf. Knowl. Discovery Data Mining*, 2003, pp. 336–345.



Kaiyu Feng received the PhD degree from Nanyang Technological University, in 2018. He is currently a research fellow with Nanyang Technological University. His current research interests include spatial data management and analysis.



Tao Guo received the PhD degree from Nanyang Technological University, in 2018. He is currently a research assistant professor with the National University of Singapore.



Gao Cong received the PhD degree from the National University of Singapore, in 2004. He is a professor with the School of Computer Engineering, Nanyang Technological University, Singapore. He previously worked at Aalborg University, Microsoft Research Asia, and the University of Edinburgh. His current research interests include geo-textual and mobility data management, data mining, social media mining, and POI recommendation.



Sourav S. Bhowmick is an associate professor with the School of Computer Science and Engineering, Nanyang Technological University. His current research interests include data management, data analytics, computational social science, and computational systems biology. He has published many papers in premium venues in these areas such as SIGMOD, VLDB, ICDE, SIGKDD, ACM MM, the *IEEE Transactions on Knowledge and Data Engineering*, the *VLDB Journal*, and *Bioinformatics*.



Shuai Ma received the PhD degrees from the University of Edinburgh, in 2010, and from Peking University, in 2004, respectively. He is a professor with the School of Computer Science and Engineering, Beihang University, China. He was a postdoctoral research fellow with the Database Group, University of Edinburgh, a summer intern at Bell Labs, Murray Hill, NJ, and a visiting researcher of MSRA. His current research interests include database theory and systems, social data and graph analysis, and data intensive computing.

▷ For more information on this or any other computing topic, please visit our Digital Library at www.computer.org/csdl.